High-Temperature Thermal Neutron Scattering Measurements and Evaluation of YH$_x$ for the Transformational Challenge Reactor[1]

Chris W. Chapman*, Kemal Ramić**, Xunxiang Hu*, Jesse Brown*, Goran Arbanas*, Douglas L. Abernathy*, Alexander I. Kolesnikov*, Matthew B. Stone*, Li (Emily) Liu***, Yaron Danon***

Oak Ridge National Laboratory, 1 Bethel Valley Road, Oak Ridge, TN, 37831
**European Spallation Source ERIC, Odarslövsvägen 113, 225 92 Lund, Sweden*
***Rensselaer Polytechnic Institute, Gaerttner LINAC Center, 3021 Tibbits Ave., Troy, NY 12180*
chapmancw@ornl.gov

INTRODUCTION

The interest in yttrium hydride for advanced reactor applications has increased in recent years [1], particularly with regard to high-temperature measurements and evaluations. While there have been extensive measurements of high-temperature thermophysical properties of YH$_x$, there are no existing high-temperature thermal neutron scattering measurements. These measurements can be used not only to calculate the thermal scattering law but also to validate various thermophysical properties.

Not only are these measurements difficult because of the extreme temperatures involved, but also traditional evaluation tools and methods can miss some key contributions at high temperature. Recent advancements in these methods, particularly the temperature dependent effective potential (TDEP) method, can account for these high-temperature effects. This paper details the continuation of temperature-dependent measurements and evaluation of yttrium hydride for the Transformational Challenge Reactor (TCR), as previously described in Chapman et al. [2], by conducting further measurements of YH$_{1.87}$ at 295, 550, 800, 900, 1000, 1100, and 1200 K at the Spallation Neutron Source (SNS) at Oak Ridge National Laboratory (ORNL).

THEORY

The TDEP method [3, 4, 5] is a collection of tools for finite temperature lattice dynamics. As other methods do, such as those cited in refs. [6, 7, 8], TDEP uses an external density functional theory code, such as VASP [9, 10, 11], to calculate the forces acting on the atoms. The main algorithm of TDEP then extracts interatomic force constants from sets of displacements and forces by fitting them to coefficients in an effective lattice dynamical Hamiltonian. From the lattice dynamics theory, we know that when an atom is displaced from its equilibrium position in the lattice, the potential energy of the lattice changes. This change in the potential energy can be modeled with a Taylor expansion of the displacement of each individual atom. We also know that the more the temperature increases, the more atoms are disordered; hence, it is not enough to just do the "frozen phonon" (0 K) calculation that is commonly used to extract the forces.

This is where the TDEP method excels. The method we used in this work, "stochastic" TDEP, or s-TDEP, can produce a thermally excited state by selecting initial atomic velocities and displacement amplitudes according to the Maxwell-Boltzmann or Bose-Einstein distributions. Such thermally initialized configurations can be used directly with a force calculator, such as VASP, and there is no need for time and computationally expensive ab initio molecular dynamics simulations to sample the Born-Oppenhaimer surface. A more detailed description of the TDEP method and its implementation in this project can be found at ref. [12] and in an upcoming paper [13].

EXPERIMENTAL RESULTS

Experimental data were gathered at the SNS from the Wide Angular-Range Chopper Spectrometer (ARCS) [14]. ARCS is a time-of-flight direct geometry spectrometer, meaning that the user selects the incident neutron energy, and the detector array tabulates the scattered spectra as a function of final energy and scattering angle. A 1 mm thin foil of YH$_{1.87}$ was encased in a thin-wall low-boron quartz tube and placed in a vanadium sample holder. This was then mounted in the furnace for the duration of the experiment. Measurements were taken at temperatures of 295, 550, 800, 900, 1000, 1100, and 1200 K. Experimental results are shown in Figs. 1–3, which depict scattering intensity as a function of energy transfer integrated over a range of measured wave-vector transfer, Q.

In the figures, we see expected features of the inelastic scattering neutron spectra: increasing temperature leads to a broadening of the peaks, as well as an increase in the magnitude of upscattering ($E < 0$). One feature of note is the shifting of the peaks, most notably in Fig. 2 between 100 and 150 meV, and in Fig. 3 between 200 and 300 meV. This shifting is caused by a change in the lattice parameters of YH$_x$ as a function of temperature.

SIMULATION RESULTS

ARCS

The experiments were simulated in MCNP6.1 [15] using the ENDF/B-VIII.0 and s-TDEP generated thermal scattering
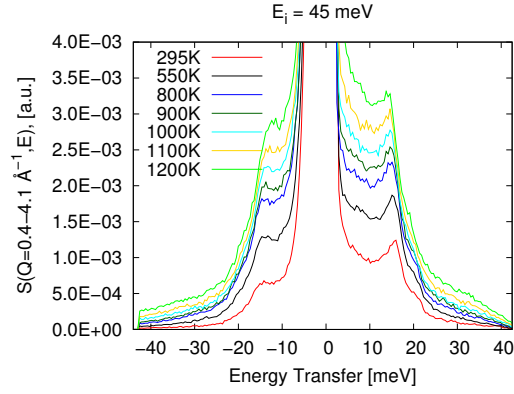
Fig. 1. Temperature comparison of Q-integrated dynamic structure factor of $YH_{1.87}$ at Ei=45 meV.
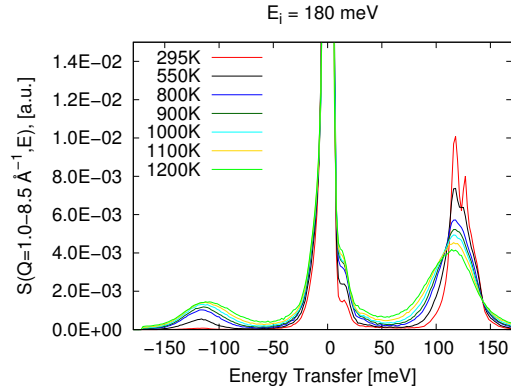

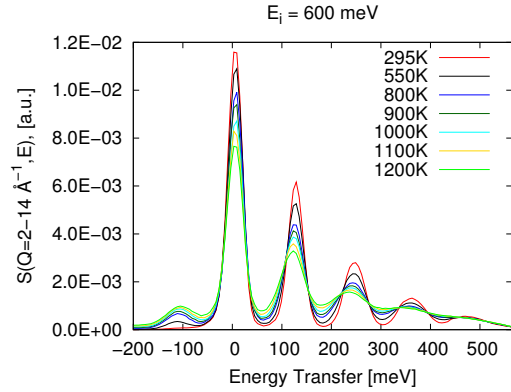Fig. 2. Temperature comparison of Q-integrated dynamic structure factor of $YH_{1.87}$ at Ei=180 meV.

Fig. 3. Temperature comparison of Q-integrated dynamic structure factor of $YH_{1.87}$ at Ei=600 meV.

libraries. The neutron beam profile for each incident energy was calculated using MCViNE [16], which was also used to calculate the detector resolution function for ARCS that was applied to the double-differential cross section (DDXS). The thermal scattering libraries were generated with NJOY2016 [17]. The comparison of the two libraries against the DDXS

measured at ARCS at 295, 900, and 1200 K experimental data at a 25° scattering angle is shown in Figs. 4–6. Each of these DDXS plots is normalized so that the maximum values are equal to 1.
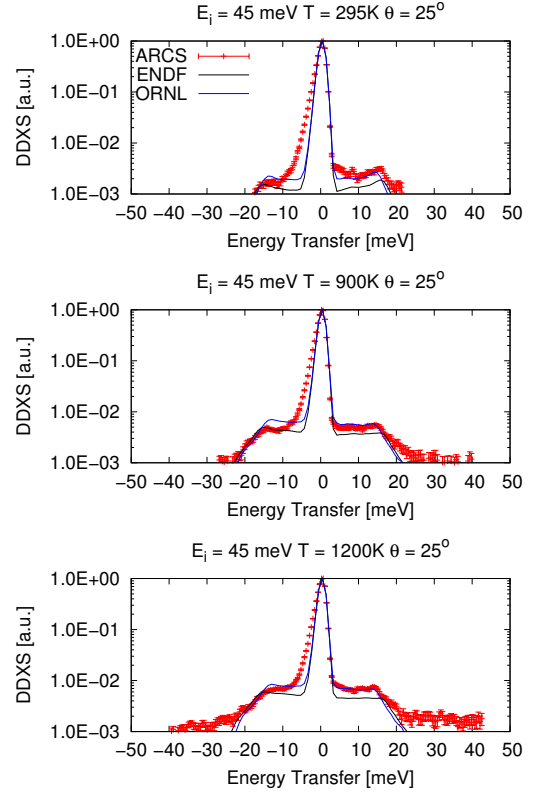

Fig. 4. DDXS comparison between ENDF/B-VIII.0 and s-TDEP against ARCS measured data at E_i=45 meV, 25° scattering angle, and temperatures of 295, 900, and 1200 K.

Figures 4 and 5 both show that, as temperature increases, the calculated acoustic peak (15 meV) shifts to better agreement with the data. This shift is most prominent in Fig. 4 at 1200 K, as the simulation data aligns almost perfectly with the experimental data between 0 and 15 meV. There is a noticeable discrepancy to the left of the elastic peak in Fig. 4, which could be related to how the detector resolution function was applied. Note that the energy resolution for a direct geometry neutron chopper spectrometer is largest at large-magnitude negative energy transfers.

In Fig. 5, the two libraries are in good agreement with each other regarding the location of the first fundamental peak in the vibrational spectrum (100–150 meV) at 295 K, but the peak shifts as temperature increases. Neither simulation appropriately handles the broadening of the fundamental mode peak, which probably results from anharmonic effects increasing with temperature.

Figure 6 shows the clearest example of shifting of the peaks in the simulated data as a function of temperature. It is most noticeable in the 1200 K simulation, where the multiphonon peaks from the ORNL evaluation align more closely with the experimental data at 237 meV and 435 meV than in
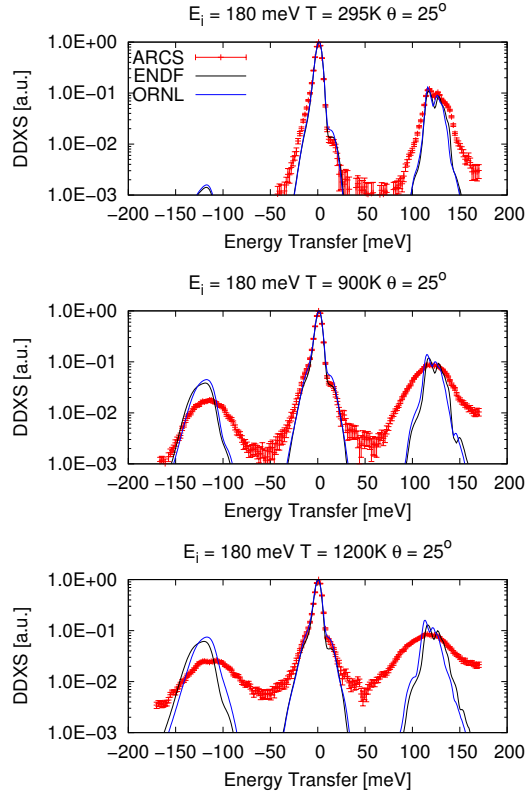
Fig. 5. DDXS comparison between ENDF/B-VIII.0 and s-TDEP against ARCS measured data at E_i=180 meV, 25° scattering angle, and temperatures of 295, 900, and 1200 K.

the ENDF evaluation.

Total Cross Section

Total neutron scattering cross sections of hydrogen in $YH_{1.87}$ as a function of temperature were also calculated using NJOY2016. A plot of the cross sections for the ORNL and ENDF evaluation at room temperature, 900 K, and 1200 K is shown in Fig. 7. Note that the ORNL evaluation at room temperature was at 295 K to match the temperature of the ARCS experiment, while the ENDF evaluation was at 293.6 K. This difference of 1.4 K was not expected to have any meaningful effect on the cross section.

The ORNL-evaluated cross section was slightly larger than the ENDF evaluated cross section, but it is uncertain at this time whether that difference has a meaningful effect on integral quantities such as criticality or reaction rates. The most noticeable difference again was the shifting of the locations of the peaks at higher temperature. It is unclear at this time which evaluation is a more faithful representation of the true experimentally measured cross section, as there are no high-temperature total scattering cross section measurements with which to compare.
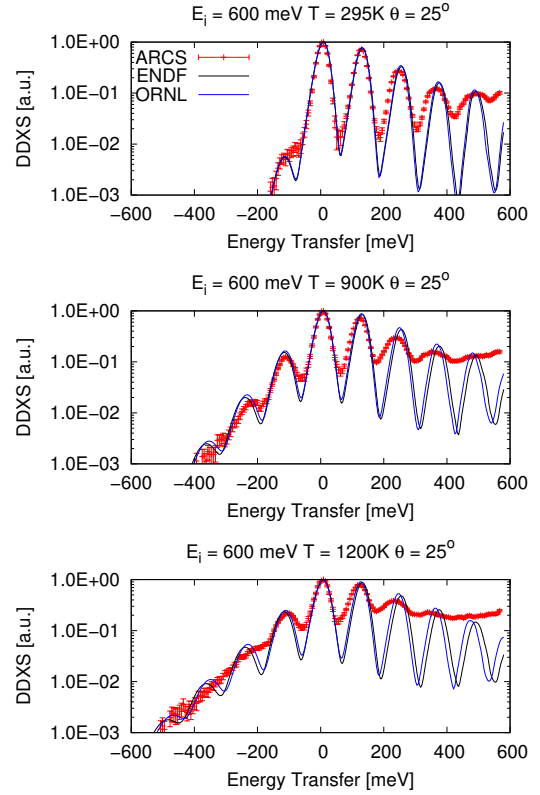

Fig. 6. DDXS comparison between ENDF/B-VIII.0 and s-TDEP against ARCS measured data at E_i=600 meV, 25° scattering angle, and temperatures of 295, 900, and 1200 K.

CONCLUSIONS AND FUTURE WORK

Thermal neutron scattering measurements of $YH_{1.87}$ at a range of temperatures were conducted at the ARCS beamline at the SNS. A preliminary evaluation based on these measurements using the s-TDEP method was compared against both these measured data and the existing ENDF/B-VIII.0 evaluation. The two evaluations exhibited some small differences from each other, with the ORNL results being slightly more closely representative of the DDXS.

Although total cross section simulated results are shown here, there are no experimentally measured temperature-dependent total cross section data for $YH_{\sim 2}$ to compare against. There are plans to measure these cross section data at the Rensselaer Polytechnic Institute Linear Accelerator in the future. Additionally, these results were simulated using MCNP6.1, which makes various approximations suitable for neutron transport, but not for replication of thermal neutron scattering experiments. Other codes like MCViNE or OCLIMAX [18] may give a more accurate set of results for comparison.
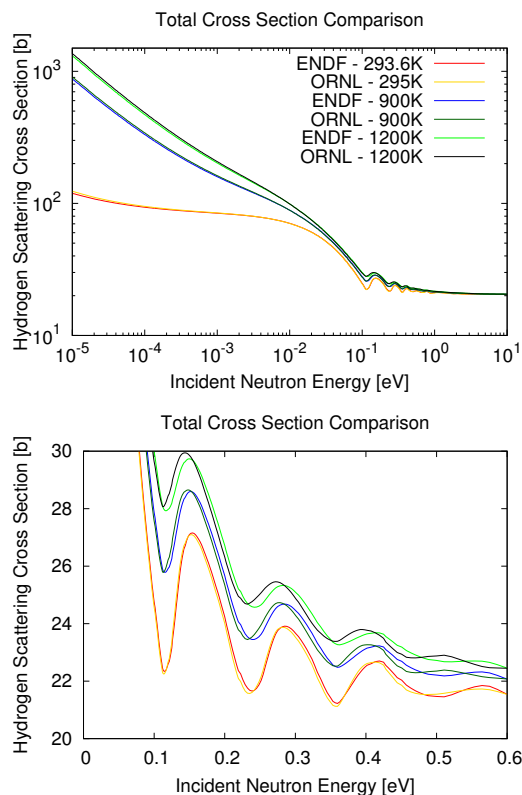
Fig. 7. Calculated hydrogen neutron scattering cross section in YH$_{1.87}$ as a function of temperature.

REFERENCES

1. V. K. MEHTA, M. W. D. COOPER, R. B. WILKERSON, D. KOTLYAR, D. V. RAO, and S. C. VOGEL, "Evaluation of Yttrium Hydride (δ-YH$_{2-x}$) Thermal Neutron Scattering Laws and Thermophysical Properties," *Nuclear Science and Engineering*, pp. 1–15 (2021).

2. C. CHAPMAN, X. HU, J. BROWN, G. ARBANAS, A. I. KOLESNIKOV, Y. CHENG, and L. DAEMEN, "Thermal Neutron Scattering Measurements of YHx for the Transformational Challenge Reactor," *Transactions of the American Nuclear Society*, **122**, 783–786 (01 2020).

3. O. HELLMAN, I. A. ABRIKOSOV, and S. I. SIMAK, "Lattice dynamics of anharmonic solids from first principles," *Phys. Rev. B*, **84**, 180301 (Nov 2011).

4. O. HELLMAN and I. A. ABRIKOSOV, "Temperature-dependent effective third-order interatomic force constants from first principles," *Phys. Rev. B*, **88**, 144301 (Oct 2013).

5. O. HELLMAN, P. STENETEG, I. A. ABRIKOSOV, and S. I. SIMAK, "Temperature dependent effective potential method for accurate free energy calculations of solids," *Phys. Rev. B*, **87**, 104111 (Mar 2013).

6. A. TOGO and I. TANAKA, "First principles phonon calculations in materials science," *Scr. Mater.*, **108**, 1–5 (Nov 2015).

7. K. PARLINSKI, "First-principle lattice dynamics and thermodynamics of crystals," *Journal of Physics: Conference Series*, **92**, 012009 (dec 2007).

8. K. PARLINSKI, "Ab initio determination of anharmonic phonon peaks," *Phys. Rev. B*, **98**, 054305 (Aug 2018).

9. G. KRESSE and J. HAFNER, "Ab initio molecular dynamics for liquid metals," *Phys. Rev. B*, **47**, 558–561 (Jan 1993).

10. G. KRESSE and J. FURTHMÃIJLLER, "Efficiency of ab-initio total energy calculations for metals and semiconductors using a plane-wave basis set," *Computational Materials Science*, **6**, *1*, 15 – 50 (1996).

11. G. KRESSE and J. FURTHMÜLLER, "Efficient iterative schemes for ab initio total-energy calculations using a plane-wave basis set," *Phys. Rev. B*, **54**, 11169–11186 (Oct 1996).

12. C. CHAPMAN, K. RAMIĆ, X. HU, J. BROWN, G. ARBANAS, A. I. KOLESNIKOV, D. L. ABERNATHY, L. L. DAEMEN, A. RAMIREZ CUESTA, Y. CHENG, M. B. STONE, L. LIU, and Y. DANON, "Thermal Neutron Scattering Evaluation of Yttrium Hydride - FY2020 Progress," (August 2020).

13. C. CHAPMAN, K. RAMIĆ, X. HU, J. BROWN, G. ARBANAS, A. I. KOLESNIKOV, D. L. ABERNATHY, L. L. DAEMEN, A. RAMIREZ CUESTA, Y. CHENG, M. B. STONE, L. LIU, and Y. DANON, "Thermal Neutron Scattering Measurements and Modeling of Yttrium-Hydrides for High Temperature Moderator Applications," *Annals of Nuclear Energy* (in review).

14. D. L. ABERNATHY, "ARCS: a wide Angular-Range Chopper Spectrometer at the SNS," *Notiziario Neutroni E Luce di Sincrotrone*, **13**, *1* (1 2008).

15. J. GOORLEY, M. JAMES, ET AL., "Initial MCNP6 Release Overview," Tech. Rep. LA-UR-13-22934, Los Alamos National Laboratory (2013).

16. J. Y. LIN, H. L. SMITH, G. E. GRANROTH, D. L. ABERNATHY, M. D. LUMSDEN, B. WINN, A. A. ACZEL, M. AIVAZIS, and B. FULTZ, "MCViNE âĂŞ An object oriented Monte Carlo neutron ray tracing simulation package," *Nuclear Instruments and Methods in Physics Research Section A: Accelerators, Spectrometers, Detectors and Associated Equipment*, **810**, 86 – 99 (2016).

17. R. MACFARLANE and A. KAHLER, "Methods for Processing ENDF/B-VII with NJOY," *Nuclear Data Sheets*, **111**, *12*, 2739–2890 (2010), Nuclear Reaction Data.

18. Y. Q. CHENG, L. L. DAEMEN, A. I. KOLESNIKOV, and A. J. RAMIREZ-CUESTA, "Simulation of Inelastic Neutron Scattering Spectra Using OCLIMAX," *Journal of Chemical Theory and Computation*, **15**, *3*, 1974–1982 (2019).